Iranian Journal of Materials Forming 9 (1) (2022) 47-54

IJMF

Online ISSN: 2383-0042

Iranian Journal of Materials Forming

Journal Homepage: http://ijmf.shirazu.ac.ir

Research Article

Wear Performance of As-Cast and Heat Treated ZK60 Mg Alloy Under Different Applied Loads

S. Abdi, M. Ardestani*, M. Tamizifar and A. Abbasi

Department of Materials Engineering, Science and Research Branch, Islamic Azad University, Tehran, Iran

ARTICLE INFO

Article history:

Received 17 November 2021
Reviewed 31 January 2022
Revised 10 February 2022
Accepted 17 February 2022

Keywords:

Zk60 alloy
Wear mechanism
Heat treatment
Wear rate
Engine

ABSTRACT

In this research, the effect of applied load on sliding wear characteristics of as-cast and heat treated ZK60 Mg alloy was investigated. The as-cast alloy was homogenized at 450°C and aged at 170°C for 10 and 35 h. The dry sliding wear behavior of the as-cast and heat treated alloys was investigated using a pin-on-disk wear test under various loads in the range of 10-160 N at a sliding velocity of 0.1 m/s for 1000 m. The worn surfaces were evaluated using scanning electron microscopy equipped with energy dispersive spectroscopy analysis. The results confirmed that the wear mechanism was dependent on the applied load. Findings revealed that the most dominant wear mechanisms under low, intermediate and high loads were oxidation, abrasion/adhesion and delamination, respectively. The heat-treated and as-cast alloys showed almost similar wear resistance under low loads, however, the heat-treated alloys showed better wear resistance than the as-cast ones at high loads.

1. Introduction

Magnesium alloys are widely used for fabrication of various industrial components such as gearboxes, frames, hubs, and struts. Low density, high specific strength, stiffness, and a great ability in damping are known as some of the significant properties of Mg alloys. However, the hexagonal close-packed (HCP) crystal structure of magnesium can lead to a lack of strength, low stiffness, poor fatigue and creep properties at high temperatures and low cold workability at room temperature [1-3]. Furthermore, the hardness, wear, and corrosion resistance of this group of alloys is not desirable. The Mg alloy components are mainly obtained through the method of casting, which is due to several economic advantages for which this method is vastly used [4-6]. Therefore, to modify mechanical properties of the magnesium alloys, some research concentrated on optimization of heat-treatment processing methods [7-9]. Solution treatment and/or aging process have been utilized to enhance the mechanical properties of Mg alloys such as ZK60 alloy [10, 11]. ZK60 is a Zr containing commercial Mg-Zn alloy, with relatively high strength and elongation which meets the demand for such mechanical properties. As known, Zr plays the main role in grain refining during solidification [12-14]. In this line of research, Kang et al. [15] investigated the microstructure changes and mechanical properties of

* Corresponding author
E-mail address: m-ardestani@srbiau.ac.ir (M. Ardestani)
https://doi.org/10.22099/IJMF.2022.42285.1204

ZK60 alloy sheets by T6 heat-treatment. The tensile strength, yield strength and elongation of the heat-treated alloys were 321 MPa, 280 MPa and 16%, respectively. Similarly, Chen et al. [16] studied the microstructure and mechanical properties of ZK60 Mg alloy under different solution treatments and artificial aging conditions. The results showed that solution treatment at 400°C for 10 h and artificial aging at 150°C for 30 h were considered as the best heat-treatment conditions to obtain a desirable combination of strength and ductility. The wear properties of some Mg alloys have been investigated in several research projects. For instance, Lim et al. studied the wear mechanism of magnesium-based composites reinforced with silicon carbide [17]. Observations showed that abrasion, oxidation, delamination, adhesion, thermal softening, and melting were the main wear mechanisms of the studied alloys. In addition, An et al. [18] studied the wear properties of $Mg_{97}Zn_1Y_2$ and AZ91 as-cast magnesium alloys. They confirmed that the optimal surface properties of $Mg_{97}Zn_1Y_2$ alloy at high load were caused due to the thermal stability of the intermetallic phase and the desired elevated temperature mechanical properties of the alloy. In another study, the results of Lopez et al. [19] on wear behavior of the ZE41A magnesium alloy showed that the wear rate increased with applied loads and reduced with sliding velocity. Jiang et al. [20] showed that the wear resistance of the extruded Mg-9Sn-3Yb was higher than that of Mg-9Sn alloy, which was due to the formation of Mg_2Sn and Mg_2(Sn, Yb) particles during the wear resistance test. Aung et al. [21] studied the wear performance of the AZ91D alloy at low sliding speeds. They showed that the wear rate was lowest and highest in oxidational and abrasive wear, respectively. In a similar vein, Zengin et al. [22] examined the tensile and wear properties of both as-cast and extruded ZK60 magnesium alloys that contained low amounts of Nd additions. They reported that, by increasing the Nd content, the wear resistance of the as-cast ZK60 alloy was modified after extrusion and was slightly elevated. Gong et al. [23] studied the effect of compressive deformation on wear characteristics of extruded ZK60 Mg alloy. They showed that the wear resistance of the alloy could be improved by pre-compression. As the ZK60 alloy has a great potential for use in the automotive industry, especially in engines as cam cover, its wear behavior is considered as a significant feature. However, to the best of our knowledge, although the effect of heat treatment on the tensile properties of ZK alloy has been investigated in previous studies [15, 16], there is no detailed research on the effect of heat treatment on the wear behavior of ZK60 alloy under different applied loads. Therefore, the present study sought to examine the wear properties of as-cast and heat treated ZK60 Magnesium alloy. The friction coefficient values were found to fluctuate with an increase in sliding speed leading to three different wear transitions.

2. Experimental Method

The ZK60 magnesium ingots with chemical composition (in wt%) of 5 Zn and 0.5 Zr (component chemical composition determined by inductively coupled plasma (ICP) method by Perkin Elemer-Optima 7300DV- device) were prepared via casting. To produce the ZK60 Mg alloy, commercially pure Mg (99.9%), Mg-50Zn and Mg-10Zr master alloys were used as the basic materials. The melting procedure was done using an induction furnace which was protected in an (Ar+3%SF6) atmosphere. At first, pure Mg was melted and then the Mg-50Zn master alloy was added to the molten Mg in a graphite crucible at 750°C. Thereafter, the desired amount of Mg-10Zr was added to the molten alloy at 760°C and held for 5 min for homogenizing the melt. Then, the molten alloy was cast into a 150°C preheated cylindrical steel mold. The bars were homogenized at 450°C for 10 h, and then quenched in water. Afterwards, the alloys were aged at 170°C for 10 and 35 h, (Fig. 1(a)). The hardness of the samples was determined via an Instron Wolpert hardness tester machine under 62.5 kgf load according to the ASTM E10 standard. The average of three hardness measurements was reported as the hardness value. The wear tests were carried out under dry sliding condition in accommodation with the ASTM G-99 standard [24], with pin-on-disc wear testing configuration using the

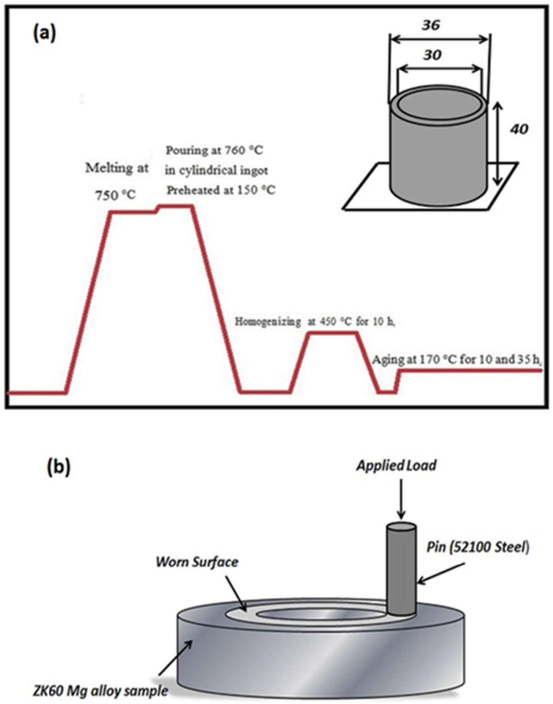

Fig. 1. (a) Schematic illustration of the applied time and temperature sequences for preparing the as-cast and heat treated alloys. (b)Symbolic representation of pin-on-disk test configuration.

ZK60 alloy as disk (7 mm × φ 30 mm) and 52100 steel as pin (Fig. 1(b)). Disk-shaped specimens were extracted by wire-electrode cutting. In minimum, two samples were tested for each wear condition. The wear tests were carried out at 10, 20, 40, 80 and 160 N loads. The sliding velocity and distance were 0.1 m/s and 1000 m, respectively. The samples were weighted before and after the wear test to determine the mass and volume loss during the test. Friction coefficient was also measured during the tests. To figure out the wear response of the material under different conditions, the Archard's law was applied as Eq. (1) [25]:

$$V/l = KW/H = kW \qquad (1)$$

where V is the wear volume, l is the sliding distance, the coefficient V/l is the wear rate, W is the applied load, H is hardness of the sample, K is the Archard's constant and k is the specific wear rate. The worn surfaces were examined by a Philips XI40 scanning electron microscope (SEM) equipped with an energy dispersive spectrometer (EDS).

3. Results and Discussion

Fig. 2 illustrates the SEM micrograph of the as-cast alloys. As shown, no porosities are observed in the microstructure and the size of the grains is mainly below 100 µm according to the microscopic investigations. The hardness of as-cast, 10 and 35 h aged specimens were 64±1, 70 ±1 and 69 ±1 HB, respectively. It has been reported that precipitation of a transition phase (i.e. β′1) is responsible for the increase in hardness after 10 h aging [15]. In addition, decreasing the hardness value after 35 h aging may also be due to a decrease in the volume percent of the transition phase volume [16]. The digital scanner images of the worn surfaces of different specimens are shown in Fig. 3. As shown, the worn surfaces of the disks, which were tested under relatively lower applied loads, appeared to be dark while those tested at higher loads had metallic sparkles.

Figs. 4(a), 4(b), and 4(c) show the sliding mass loss, specific wear rate (k), and friction coefficient as a function of normal force, respectively. The lateral wear force was measured by a load cell installed on the wear test machine and the ratio of lateral force to the applied force was reported by the software as the friction coefficient. The load cell was calibrated before each wear test. Furthermore, as it can be seen, the mass loss increased with a low rate due to an increase in the applied load up to 40 N. Additionally, further increase in the applied led to more increase in the wear rate. By

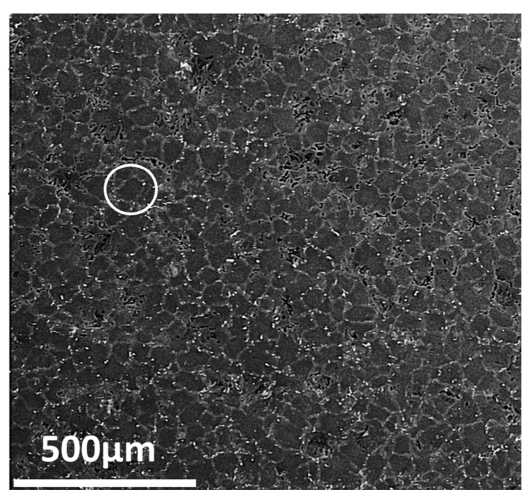

Fig. 2. SEM micrograph of the as-cast samples. A typical grain has been encircled.

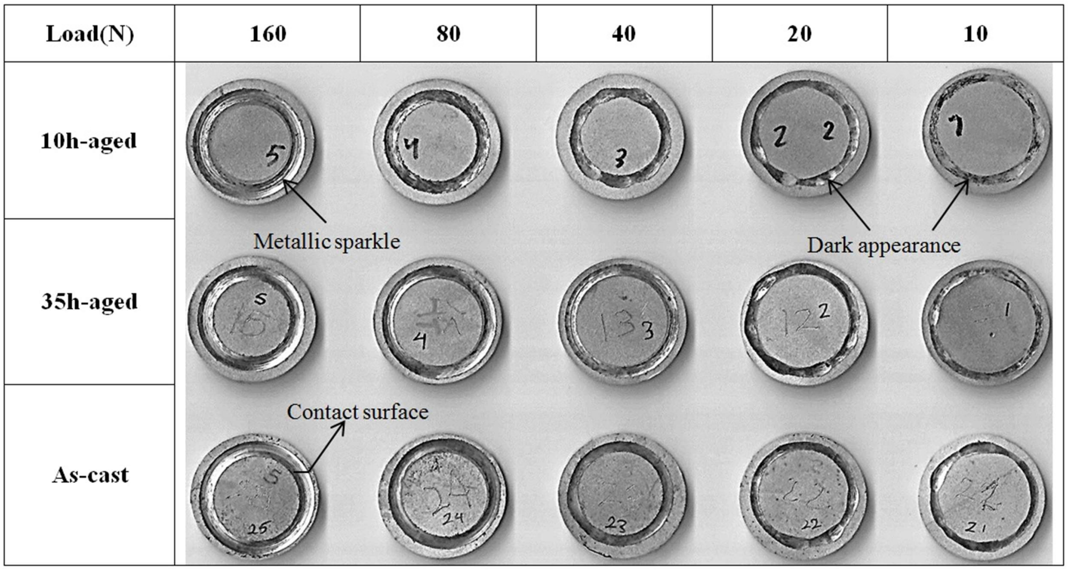

Fig. 3. Digital scanner images of the worn specimens. The worn surfaces have become wider at high loads. (The diameter of the samples is 30 mm).

increasing the load, the worn surface widening with respect to the theoretical surface, lead to an increase of the frictional force between two sliding surfaces. The expanded real contact surface and more frictional force led to more wear rate, as shown in Fig. 4. Therefore, after a critical load (40 N) a sharp increase in the mass loss could also be observed. As shown in this diagram, the heat-treated alloys showed better wear resistance at high loads, in comparison with the as-cast ones. In all these samples, friction coefficient at high loads was less than that of low and intermediate loads, indicating a change in wear mechanism.

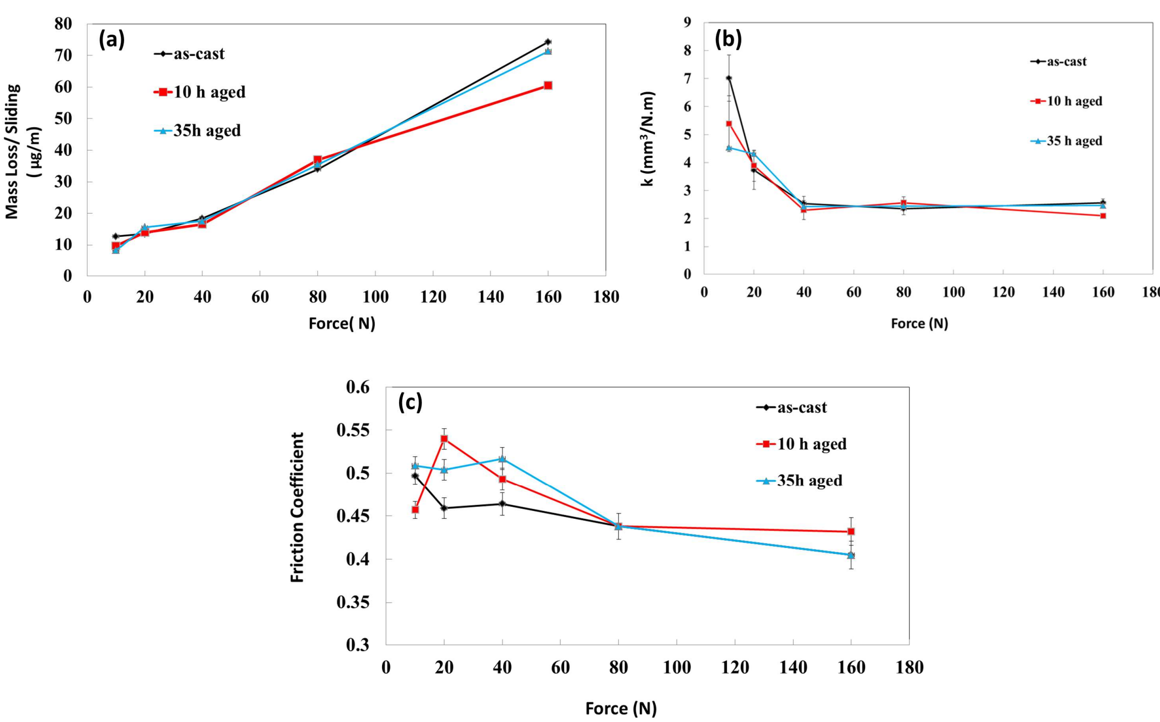

Fig. 4. Variation of: (a) mass loss/sliding, (b) specific wear rate, and (c) friction coefficient as a function of applied load.

Figs. 5(a), 6(a) and 7(a) show the SEM micrographs of the worn surfaces of different samples at 10 N. The presence of strong oxygen peak in the corresponding typical EDS result of the wear track and particles confirmed that the dominant wear mechanism of the samples was oxidation. The heat created by friction during sliding was the reason of surface oxidation. By erosion in result of the oxide components removal, during sliding, oxidation residues filled the valleys of disk surface and compressed it as a protective layer. Therefore, straight contact between two metals was restricted and the minimum amount of wear occurred [20, 21]. In this sense, An et al. [18] concluded that the deep oxide layer protected the sliding surface efficiently; therefore, light wear conditions with low wear rates were observed. Since the oxidation properties of the alloy have not been significantly changed with heat treatment, no significant differences have been observed in the oxidation mechanism between the as-cast and the heat treated samples. In addition, increasing the aging time from 10 h to 35 h has not led to major changes in surface oxidation during wear. Therefore, at low loads, similar wear properties could be reported in heat-treated parts at 10 h and 35 h. The presence of the oxidative wear is the oxidation sensitivity of Mg alloys, which increases with the use of frictional heat due to slip. The presence of this oxidation layer prevents metal contact and leads to a low wear rate. Friction occurs in this mechanism between the oxide layer and the pin; therefore, the amount of friction coefficient is a function of the behavior of these two levels. As it can be seen in Fig. 4(c), the friction coefficient decreases clearly by increasing the applied load after 40 N, indicating the destruction of the oxide layer by increasing the applied load. Figs. 5(b), 6(b) and 7(b) show the worn surface of different specimens under 20 N load. There are many rows of aligned grooves on the worn surfaces, which is an evidence of abrasion mechanism. These lines are usually formed by the hard particles created in the pin. The movement of these particles on the surface has caused the removal of material along its path on the surface of the Mg alloy [18]. The grooves formation is mainly the result of hard particles formation between the pin and the disc [19]. Aung et al. [21] concluded that abrasive wear caused deformation of the surface and created damage in deep grooves in the sliding direction.

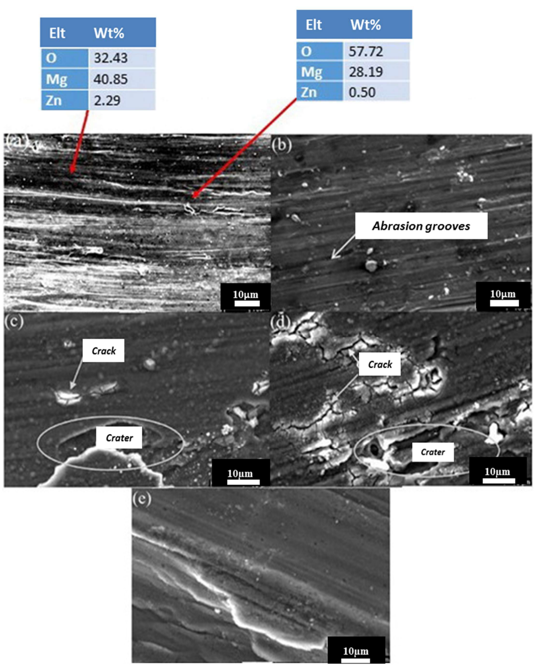

Fig. 5. The worn surfaces of as-cast samples in different loads, (a) 10 N, (b) 20 N, (c) 40 N, (d) 80 N, (e)160 N. The EDS analysis results of the particle and wear track which have been shown by arrows are given.

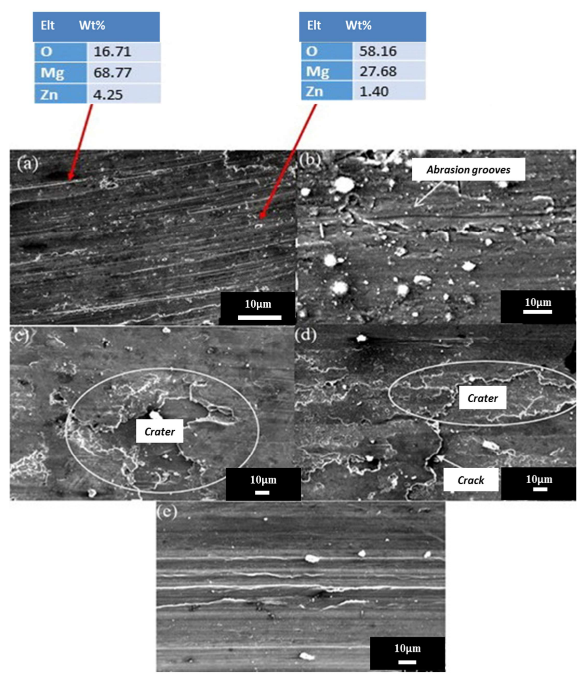

Fig. 6. The worn surfaces of the 10 h aged samples in different loads, (a) 10 N, (b) 20 N, (c) 40 N, (d) 80 N, (e) 160 N. The EDS analysis results of the particle and wear track which have been shown by arrows are given.

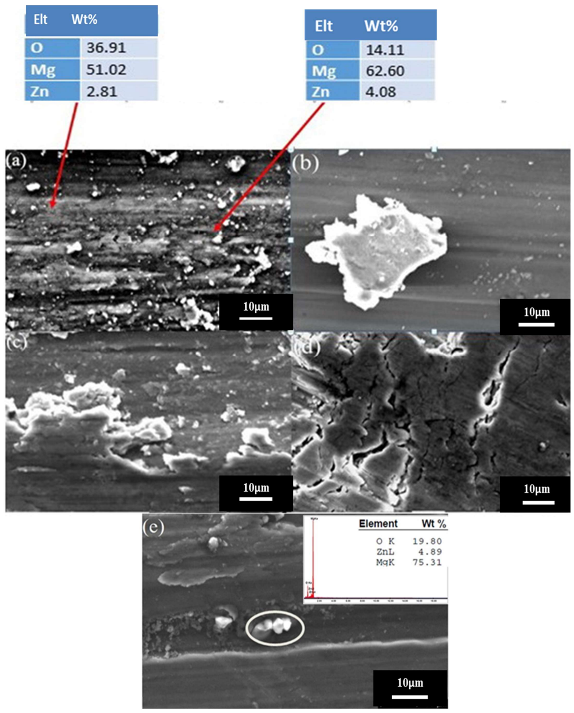

Fig. 7. The worn surfaces of the 35 h aged samples in different loads, (a) 10 N. The EDS analysis results of the particle and wear track which have been shown by arrows are given, (b) 20 N, (c) 40 N, (d) 80 N, (e) 160 N. The EDS analysis result of the particle around which a circle drawn is given.

This wear mechanism removed materials from the surface, which was the predominant wear mechanism for lower loads, along with the oxidation mechanism. As shown in Fig. 4(c), the friction coefficient of as-cast samples is more than the heat-treated ones due to more debris of the worn surface at high loads. Due to this fact that heat treatment has led to an increase in hardness, grooves with less depth have been observed in the heat-treated samples. In addition, in samples with 10 h aging, abrasion resistance is higher than 35 h aged samples because of hardness reduction as a result of over aging. Figs. 5(c), 5(d), 6(c), 6(d), 7(c), and 7(d) show the worn surfaces of as-cast and aged samples tested at 40 and 80 N of applied load. In these cases, some small craters with 20-50 µm in length formed and spread on the worn surfaces. Generally, adhesion occurs because of micro welding of the contact surfaces. Because of sliding between surfaces of the two materials at the wear contact surface, shear stress can be seen in the micro-joint and the softer material breaks. In the present case, the magnesium alloy is softer than the steel pin, resulting in a small crater appearing on the magnesium surface because of adhesion and removal of the material to the pin. The friction coefficient in this mechanism did not show a significant variation due to the surface adhesion, compared to the abrasive wear. Furthermore, large craters could be seen on the worn surfaces due to the delamination mechanism (Fig. 5(c) and 5(d)). The size of the craters ranged from 10 to 40 µm in length. It has been shown that the change of the crater size was related to the change of the applied load [18]. In general, delamination is distinguished by the formation of cracks perpendicular to the sliding direction, causing separation of the sheet-like piece from the worn material. Furthermore, this wear mechanism is related to fatigue, in which repeated slippage causes subsurface cracks, cracks grow gently and cut into the surface in due course [19, 21]. Furthermore, Figs. 5(c) and 5(d) show how crack nucleates and propagates along the oxides formed at the surface of the worn disc, which are in good agreement with the earlier findings [18-21]. Moreover, Fig. 7(d) shows a series of cracks which are approximately perpendicular to the direction of the slip. In this regard, Das et al. [27] noted that delamination is caused by propagation of cracks, beneath the surface. When such subsurface cracks join the wear surface, delamination becomes the predominant wear mechanism. Additionally, by increasing the applied load from 40 to 80 N, decrease in friction coefficient occurs, indicating change in wear mechanism from adhesion to delimitation (Fig. 4(c)). Plastic deformation was observed at high loads (Figs. 5(e), 6(e) and 7(e)), as it has been reported in many magnesium alloys [18-21]. The main attribute of plastic deformation is the very large deformation of the surface and the local melting of the material, which causes extensive surface damage, however not necessarily a large amount of loose debris is formed in the process. During wear tests at high loads, the material undergoes extensive plastic deformation, resulting in its brittle parts breaking. According to Fig. 5(d), most of the cracks can be seen in the oxidized zones that show oxidation related to the deformed zone embrittlement. As what takes place in delamination mechanism, cracks nucleate and progress the length of the oxide layer. The severe plastic deformation causes higher wear rate with increase in load and speed. In this respect, Lopez et al. [19] announced large surface damage due to plastic deformation of the material layers conjoining to the contact surface at higher loads. As the temperature increased, the yield strength obviously decreased, and the alloy softened. As a result, the materials became susceptible to plastic deformation and spread in the direction of slip and move sideways from the contact surface. According to the EDS analysis results of the worn surface, no oxidation could be seen (Fig. 7(e)). As shown in Fig. 4(c), the lowest friction coefficient can be related to this condition. In other words, at high temperatures, deformation is easier. At low loads, an oxide layer forms on its surface. Under these conditions, oxidation played a crucial role in wear and heat-treatment and did not lead to any major changes in the wear characteristics of ZK60 Mg alloys. By increasing the load, the delamination mechanism appeared on the worn surface, and when the load was more than 40 N, a sharp change in the slope of diagram could be seen. At the intermediate and high loads, the delamination became a dominant mechanism.

As study revealed, the progression of under surface cracks caused the limited plastic deformation of the Mg alloys, causing large platelets to separate from the alloy; however, they appeared in a few regions. The wear rate increased slightly compared to the previous region and the friction coefficient was fully stable. Plastic deformation in high loads was the dominated mechanism at high loads. In this regime, massive surface deformation and local melting of material occurred. Due to the improvement of hardness and mechanical properties of alloy after heat-treatment, heat-treated ZK60 Mg alloys showed less wear rate at high loads.

As described above, k is the specific wear rate amount in different test conditions (Fig. 4(b)). By increasing the load, the specific wear rate was decreased. The reason of this phenomenon is related to changing the wear mechanism from oxidation to plastic deformation. Since magnesium alloys are sensitive to oxidation, k is relatively high at low loads. By changing the wear mechanism at high loads, the plastic deformation was activated, and the k value decreased. However, the 10 h aged samples show lower k value because of their better mechanical properties (higher hardness).

4. Conclusion

In this research, the effects of age hardening heat-treatment and the value of applied load on wear characteristics of ZK60 Magnesium as-cast alloy were investigated using pin-on-disc wear test. The following results were obtained:

1. Enhancing the load from 10 to 160 N led to a significant increase in the sliding mass loss. The friction coefficients at high loads were less than those of low and intermediate loads, which was due to the change in the wear mechanism.
2. The most dominant wear mechanisms at low loads were oxidation. In such conditions, the wear resistances of as-cast and heat-treated alloys was revealed to be similar due to the formation of metal mixed oxide layers on the worn surfaces.
3. The wear mechanism was abrasion/adhesion and delamination at medium and high loads, respectively. Features of plastic deformation were observed on the worn surfaces by increasing the applied load. In these conditions, the wear resistance of the heat-treated alloys was higher than that of the as-cast ones.

Acknowledgments

The authors wish to thank the Sapco Company for assistance with wear test and SEM analysis. They are further grateful to Dr. M. Tayebi for assistance in providing the master alloys.

5. References

[1] J. Song, F. Pan, B. Jiang, A. Atrens, M.X. Zhang, Y. Lu, A review on hot tearing of magnesium alloys, *Journal of Magnesium and Alloys*, 4(3) (2016) 151-172.

[2] S.D. Babu, P. Sevvel, R.S. Kumar, Simulation of heat transfer and analysis of impact of tool pin geometry and tool speed during friction stir welding of AZ80A Mg

alloy plates, *Journal of Mechanical Science and Technology*, 34(10) (2020) 4239-4250.

[3] M. Paidar, D. Bokov, S. Mehrez, O.O. Ojo, V.V. Ramalingam, S. Memon, Improvement of mechanical and wear behavior by the development of a new tool for the friction stir processing of Mg/B4C composite, *Surface and Coatings Technology*, 426 (2021) 127797.

[4] K.H. Jung, S. Lee, Y.B. Kim, B. Ahn, E.Z. Kim, G.A. Lee, Assessment of ZK60A magnesium billets for forging depending on casting methods by upsetting and tomography, *Journal of Mechanical Science and Technology,* 27(10) (2013) 3149-3153.

[5] K. Singh, G. Singh, H. Singh, Review on friction stir welding of magnesium alloys, *Journal of Magnesium and Alloys*, 6(4) (2018) 399-416.

[6] E. Karakulak, A review: Past, present and future of grain refining of magnesium castings, *Journal of Magnesium and Alloys,* 7(3) (2019) 355-369.

[7] A.G. Beer, M.R. Barnett, Microstructure evolution in hot worked and annealed magnesium alloy AZ31, *Materials Science and Engineering: A*, 485(1-2) (2008) 318-324.

[8] D.K. Xu, L. Liu, Y.B. Xu, E.H. Han, The effect of precipitates on the mechanical properties of ZK60-Y alloy, *Materials Science and Engineering: A*, 420(1-2) (2006) 322-332.

[9] N. Balasubramani, U.T.S. Pillai, B.C. Pai, Optimization of heat treatment parameters in ZA84 magnesium alloy, *Journal of Alloys and Compounds*, 457(1-2) (2008) 118-123.

[10] H. Chen, S.B. Kang, H. Yu, J. Cho, H.W. Kim, G. Min, Effect of heat treatment on microstructure and mechanical properties of twin roll cast and sequential warm rolled ZK60 alloy sheets, *Journal of Alloys and Compounds*, 476(1-2) (2009) 324-328.

[11] J.H. Cho, M.Y. Jin, H.W. Kim, S.B. Kang, Microstructure and mechanical properties of ZK60 alloy sheets during aging, *Materials Science Forum*, 558 (2007) 159-164.

[12] P. Saha, S. Viswanathan, Engineering an efficient zirconium-based grain refiner for magnesium alloys, *International Journal of Metalcasting*, 1(4) (2010) 70-71.

[13] J. Chen, L. Tan, K. Yang, Effect of heat treatment on mechanical and biodegradable properties of an extruded ZK60 alloy, *Bioactive Materials*, 2(1) (2017) 19-26.

[14] D.H. StJohn, M.A. Qian, M.A. Easton, P. Cao, Z. Hildebrand, Grain refinement of magnesium alloys. *Metallurgical and Materials Transactions A*, 36(7) (2005) 1669-1679.

[15] S.B. Kang, J.H. Cho, H.W. Kim, Y.M. Jin, Effect of heat treatment on microstructure and mechanical properties in ZK60 alloy sheet, *Materials Science Forum*, 567 (2008) 361-364.

[16] X.H. Chen, X.W. Huang, F.S. Pan, A.T. Tang, J.F. Wang, D.F. Zhang, Effects of heat treatment on microstructure and mechanical properties of ZK60 Mg alloy, *Transactions of Nonferrous Metals Society of China*, 21(4) (2011) 754-760.

[17] C.Y.H Lim, S.C. Lim, M. Gupta, Wear behavior of SiCp-reinforced magnesium matrix composites, *Wear*, 255(1-6) (2003) 629-637.

[18] J. An, R.G. Li, Y. Lu, C.M. Chen, Y.C. Xu, X. Chen, L.M. Wang, Dry sliding wear behavior of magnesium alloys, *Wear*, 265(1-2) (2008) 97-104.

[19] A.J. López, P. Rodrigo, B. Torres, J. Rams, Dry sliding wear behavior of ZE41A magnesium alloy, *Wear*, 271(11-12) (2011) 2836-2844.

[20] J. Jiang, B.I. Guangli, Z.H.A.O. Lei, L.I. Rongguang, L.I.A.N. Jianshe, Z. Jiang, Dry sliding wear behavior of extruded Mg-Sn-Yb alloy, *Journal of Rare Earths*, 33(1) (2015) 77-85.

[21] N.N. Aung, W. Zhou, L.E. Lim, Wear behavior of AZ91D alloy at low sliding speeds, *Wear*, 265(5-6) (2008) 780-786.

[22] H. Zengin, Y. Turen, M.E. Turan, Tensile and wear properties of as-cast and as-extruded ZK60 magnesium alloys containing minor Nd additions, *Materials Research Express*, 6(8) (2019) 086528.

[23] G. Gong, G. Huang, L. Huang, F. Pan, B. Jiang, Effect of compressive deformation on wear property of extruded ZK60 magnesium alloy, *Tribology Transactions*, 62(1) (2019) 1-7.

[24] P.J. Blau, K.G. Budinski, Development and use of ASTM standards for wear testing, *Wear*, 225 (1999) 1159-1170.

[25] J. Archard, Contact and rubbing of flat surfaces, *Journal of applied physics*, 24(8) (1953) 981-988.

[26] H. Dong, Surface engineering of light alloys: Aluminium, magnesium and titanium alloys, Elsevier, 2010.

[27] S. Das, S.V. Prasad, T.R. Ramachandran, Microstructure and wear of cast (Al-Si alloy)-graphite composites, *Wear*, 133(1) (1989). 173-187.